



OPEN Long-term systemic androgen deprivation partially modulates neuroinflammation in male *App^{NL-G-F/NL-G-F}* mice

Kasumi Maekawa^{1,2}, Akira Sobue^{1,2,3}, Okiru Komine^{1,2}, Yuko Saito⁴, Shigeo Murayama^{5,6}, Takaomi C. Saido⁷, Takashi Saito^{1,8} & Koji Yamanaka^{1,2,9,10,11}✉

Alzheimer's disease (AD) is the leading neurodegenerative disease manifesting cognitive impairment. Its procession is regulated by activated glial cell-mediated neuroinflammation. Although estrogen deprivation is a known risk factor for AD in females, the impact of androgen deprivation on AD pathology in males, particularly regarding neuroinflammation, remains unclear. This study investigates the effects of long-term systemic androgen deprivation on AD pathology, including glial cell-specific gene expression, amyloid β (A β) pathology, and cognitive function in male castrated *App^{NL-G-F/NL-G-F}* (App) mice. We found significantly reduced androgen receptor (AR/Ar) expression levels in the precune of male patients with early AD pathology and isolated brain microglia of male App mice compared with their nonpathological controls. In castrated App mice, microglial *Tnf* and *Il6* and astrocytic *Socs3* were downregulated, indicating that androgens may promote inflammation in the brain. However, A β accumulation and cognitive function were unaffected. These results suggest that although systemic androgen deprivation modulates neuroinflammation, the changes are insufficient to alter the AD phenotype or pathology in male App mice.

Keywords Alzheimer's disease, Microglia, Neuroinflammation, Androgen, Castration

Alzheimer's disease (AD), the most common cause of dementia, is a neurodegenerative disease characterized by amyloid β (A β) aggregation, hyperphosphorylated tau, and progressive neuronal loss. Previous genome-wide association studies support the involvement of neuroinflammation in AD pathology^{1–3}, driven by activated glial cells (microglia and astrocytes) and infiltrating peripheral immune cells^{4,5}.

Microglia, the innate immune cells of the central nervous system (CNS), continuously monitor the CNS environment^{6,7}. When activated, microglia maintain homeostasis by releasing pro- and anti-inflammatory cytokines and clearing abnormal protein aggregates via phagocytosis^{8–10}. Disease-associated microglia (DAM), the novel subtype of activated microglia, have been identified in 5xFAD AD model mice¹¹. Our previous research revealed that activated microglia in various neurodegenerative mouse models exhibit reduced expression of homeostatic microglial genes in correlation with the degree of neuronal loss, along with uniformly upregulated DAM gene expression regardless of neurodegeneration severity¹². Additionally, microglia interact with astrocytes which regulate CNS homeostasis in diverse functions¹³. For example, the combination of proinflammatory cytokines (TNF, IL-1 α , and C1q) released by activated microglia induce neurotoxic (A1) reactive astrocytes in

¹Department of Neuroscience and Pathobiology, Research Institute of Environmental Medicine, Nagoya University, Aichi 464-8601, Japan. ²Department of Neuroscience and Pathobiology, Nagoya University Graduate School of Medicine, Aichi 466-8550, Japan. ³Medical Interactive Research and Academia Industry Collaboration Center, Research Institute of Environmental Medicine, Nagoya University, Aichi 464-8601, Japan. ⁴Department of Neuropathology, Tokyo Metropolitan Institute for Geriatrics and Gerontology, Tokyo 173-0015, Japan. ⁵Brain Bank for Aging Research, Tokyo Metropolitan Geriatric Hospital and Institute of Gerontology, Tokyo 173-0015, Japan. ⁶Brain Bank for Neurodevelopmental, Neurological and Psychiatric Disorders, United Graduate School of Child Development, Osaka University, Osaka, Japan. ⁷Laboratory for Proteolytic Neuroscience, RIKEN Center for Brain Science, Saitama 351-0198, Japan. ⁸Department of Neurocognitive Science, Institute of Brain Science, Nagoya City University Graduate School of Medical Sciences, Aichi 467-8601, Japan. ⁹Institute for Glyco-core Research (iGCORE), Nagoya University, Aichi, Japan. ¹⁰Center for One Medicine Innovative Translational Research (COMIT), Nagoya University, Aichi, Japan. ¹¹Research Institute for Quantum and Chemical Innovation, Institutes of Innovation for Future Society, Nagoya University, Aichi, Japan. ✉email: yamanaka.koji.p4@f.mail.nagoya-u.ac.jp

vitro^{13,14}. Considering prior studies on neuroinflammation in AD^{4,5}, regulating glial activation and subsequent neuroinflammation may modulate AD pathology and phenotype.

Sex differences in AD incidence are well recognized, with females having around a 1.5 times higher risk of developing AD compared with males^{15–17}. This is likely linked to the sharp decline in estrogen (mainly estradiol) levels during perimenopause¹⁸. Indeed, *in vivo* studies have shown that ovariectomy exacerbates cognitive impairment, neuronal loss, β -site APP cleaving enzyme 1 (BACE1) activity, and A β aggregation in female AD model mice^{19–21}. Although the role of estrogens in AD pathomechanisms has been extensively studied, less focus has been placed on androgens, such as testosterone and its metabolite dihydrotestosterone (DHT). Previous studies have reported lower brain and serum testosterone levels in male patients with AD compared to those without cognitive impairment^{22,23}, suggesting that androgen deprivation may be a risk factor for AD in males. Additionally, clinical studies examining the link between androgen deprivation therapy (ADT) for prostate cancer and dementia/AD have produced mixed results. Some studies found a positive association^{24–30}, whereas others did not^{31–35}, leaving the association between AD and androgen deprivation unresolved.

Only a few studies have explored how androgen deprivation affects AD pathophysiology using genetic AD mouse models. These studies showed that castration exacerbated cognitive impairment, A β aggregation, and synaptic dysfunction, and that DHT treatment ameliorated these effects^{36,37}. However, they did not address whether androgens influence specific glial cell types and neuroinflammation. To better understand the relationship between long-term systemic androgen deprivation and AD pathophysiology, particularly neuroinflammation, we investigated the effects of castration on glial cell-specific gene expression, A β pathology, and cognitive function in genetic AD mouse models that recapitulate the early-stage A β pathology in humans.

Methods

Human postmortem brain tissue

To determine androgen receptor (AR) mRNA expression levels, the same postmortem brains as obtained and analyzed in our previous study¹² were used. As described previously, the postmortem brains from 25 individuals, including non-AD (control; $n=14$) and patients with early AD pathology (mild AD; $n=11$), were obtained by autopsy with informed consent at the Brain Bank for Aging Research, Tokyo Metropolitan Geriatric Hospital and Institute of Gerontology. These brains were classified and selected based on Braak staging³⁸. The detailed information on human samples is shown in **Supplementary Table 1**. Tissues were dissected from the precuneus and immediately frozen in liquid nitrogen and stored at -80°C before use for RNA extraction. The use of human postmortem brain tissue was approved by the Ethics Committees at Nagoya University (approval number #399) and Tokyo Metropolitan Institute. All methods were carried out in accordance with relevant guidelines and regulations.

Experimental animals

Heterozygous $App^{+/NL-G-F}$ mice carrying the *App* gene with humanized A β sequence and three familial AD mutations (Swedish, Arctic and Beyreuther/Iberian) were established by a knock-in strategy³⁹. Homozygous $App^{NL-G-F/NL-G-F}$ (*App*) mice were obtained by crossbreeding of $App^{+/NL-G-F}$ mice, and were maintained by inbred lines with C57BL/6J genetic background. C57BL/6J mice as wild-type (WT) mice were purchased from Nihon CLEA Co. (Tokyo, Japan).

For castration study, 4-month-old male WT and *App* mice were randomly assigned to sham-operation (Sham) group or castration (Cast) group as follows: Sham-WT mice, Cast-WT mice, Sham-*App* mice, and Cast-*App* mice. Mice were operated under three types of mixed anesthesia (medetomidine: midazolam: butorphanol = 0.75: 4.0: 5.0 mg/kg). Sham-operation consisted only of peritoneal incision and suturing, while castration consisted of bilateral removal of testes and epididymides. Mice were used for behavioral testing at 18 months of age, after which their brains, blood, spleens, testes (sham mice only), and seminal vesicles (SVs; sham mice only) were collected for the following experiments.

All mice were maintained under a controlled environment (12 h light/dark-cycle; $23 \pm 1^{\circ}\text{C}$; $50 \pm 5\%$ humidity) with free access to food and water throughout the experiments. Animals were treated in compliance with the guidelines established by the Institutional Animal Care and Use Committee of Nagoya University. The experiments using genetically modified mice were approved by the Animal Care and Use Committee and the recombinant DNA experiment committee of Nagoya University (approval numbers RIEM240025 and RIEM240026, and #143, respectively). In addition, all methods are reported in accordance with ARRIVE guidelines.

Isolation of glial cells from mouse brain

Microglia and astrocytes were isolated from 8- and 18-month-old male WT and *App* mice via magnetic-activated cell sorting (MACS). Mice were deeply anesthetized by an overdose of three types of mixed anesthesia (medetomidine, midazolam, and butorphanol) and were transcardially perfused with phosphate-buffered saline (PBS), and then the cerebral cortex was dissected and dissociated at 37°C for 30 min using Neural Tissue Dissociation Kit – Postnatal Neurons (Miltenyi Biotec, Bergisch-Gladbach, Germany) with gentleMACS Octo Dissociator with Heaters (Miltenyi Biotec). Myelin debris was removed using Myelin Removal Beads II (Miltenyi Biotec) and the negative fraction was used for the next step. This fraction was incubated with anti-CD16/CD32 antibodies (Thermo Fisher Scientific, Waltham, MA, USA) for blocking Fc receptors. Microglia were isolated using anti-CD11b (Microglia) MicroBeads (Miltenyi Biotec), and astrocytes were isolated using anti-ACSA-2 MicroBeads (Miltenyi Biotec). All isolations were performed using autoMACS pro separator (Miltenyi Biotec) through LS column (Miltenyi Biotec).

Quantitative analysis of mRNA

To determine *AR/Ar* mRNA expression levels or glial cell-specific gene expression levels, total RNA was extracted from the precuneus of frozen postmortem brain using mirVana miRNA Isolation Kit (Thermo Fisher Scientific), and from the cerebral cortex of 8- or 18-month-old male WT and App mice using TRIzol reagent (Invitrogen, CA, USA), according to the manufacturer's instructions. Total RNA from MACS-isolated glial cells was extracted using RNeasy Micro Kit (Qiagen, Hilden, Germany) according to the manufacturer's instructions.

Complementary DNA (cDNA) was synthesized from 16 ng (astrocytes), 16 or 24 ng (microglia), 160 or 500 ng (cerebral cortex), or 25 ng (human precuneus) of each total RNA using the PrimeScript RT reagent Kit (Perfect Real Time) (TaKaRa Bio, Kusatsu, Japan).

Quantitative PCR (qPCR) reactions were performed with the TB Green Fast qPCR Mix (TaKaRa Bio) using Thermal Cycler Dice Real Time System III (TaKaRa Bio) and the following PCR cycle: 1 cycle at 95 °C for 30 s, 60 cycles at 95 °C for 5 s and 60 °C for 10 s, and a dissociation step of 95 °C for 15 s, 60 °C for 30 s, and 95 °C for 15 s. The expression levels of each target gene were normalized to the expression levels of *GAPDH* (for human samples) or *Actb* (for mouse samples) in each sample. The sequences of the primers used for qPCR are shown in **Supplementary Table 2**.

Immunofluorescence

Mice were deeply anesthetized as described above and transcardially perfused with PBS followed by 4% paraformaldehyde (PFA)/PBS. Brains were dissected, postfixed in the same fixative, and cryoprotected in 30% (w/v) sucrose/PBS. Coronal brain sections were cut every 20 µm thickness and fixed in 4% PFA/PBS for 5 min. Depending on the target, sections were permeabilized with 0.3% Triton X-100/PBS for 1 h or antigen retrieved with HistoVT One (Nacali Tesque, Kyoto, Japan) for 40 min at 70 °C. After incubation in blocking solution (5% goat serum/0.3% Triton X-100/PBS) for 1 h, sections were incubated with a combination of the following antibodies: rabbit anti-IBA1 (#019-19741, 1:500, Wako, Osaka, Japan), mouse anti-human amyloid β (N) (82E1) (#10326, 1:200, IBL, Japan), rat anti-CD68 (FA-11) (#MCA1957T, 1:1000, Bio-Rad, USA) and rabbit anti-BACE1 (D10E5) (#5606, 1:100, Cell Signaling Technology, Danvers, MA, USA) at 4 °C overnight. After washing with PBS, sections were incubated with fluorescence-conjugated secondary antibodies (goat anti-rabbit, anti-mouse IgGs or goat anti-rat, 1:1000, Thermo Fisher Scientific) and DAPI (#D1306, 1:2000, Invitrogen) for nuclear staining at room temperature for 1 h. After washing with PBS, sections were mounted on slides with Fluoromount/Plus (#K048, Diagnostic BioSystems, Pleasanton, CA, USA). Images were acquired using a confocal microscope (LSM900, Carl Zeiss, Oberkochen, Germany) and quantitative analysis of the images was performed using ImageJ (National Institutes of Health, USA). For quantification, the images were obtained in the 638.90 µm square areas indicated by the white squares in Supplementary Fig. 4a. One to two square areas per slice × 3 slices per mouse were analyzed. For quantitative analysis of CD68 staining, the Aβ-positive area was defined as the "Aβ plaque" and the region including the Aβ plaque and the area within 10 µm from the plaque boundary was defined as "surrounding Aβ plaque". The number of CD68/IBA1 double-positive staining surrounding Aβ plaque was subsequently counted.

Barnes maze test

A series of Barnes maze tests were conducted on a white circular platform (90 cm in diameter) with 12 holes (5 cm in diameter) evenly spaced around the perimeter under 540 lx. A black escape box (10 × 14 × 5 cm) was placed under the target hole. Four distal visual cues were placed around the test platform. The experimenter remained adjacent to the test room and observed the test via video recorded using a camera mounted on a table. All data were collected using Smart 3.0 (Panlab). Mice were transported to the test platform using a white carrying box (10.5 × 10.5 × 10.5 cm). After each trial, the escape box and the carrying box were cleaned with distilled water, and the test platform was carefully cleaned with ethanol. Mice were habituated to the test environment for at least 1 h each day prior to the start of the trial.

For the initial five days, mice were trained to learn the position of the target hole leading into the escape box by using some visual cues. Mice were individually transported and placed in the carrying box located in the center of the test platform for 15 s. After removing the carrying box, mice were allowed to explore on the test platform for 5 min. The trial ended when mice entered the escape box, and mice were habituated for 1 min before returning to the home cage. When time was up, mice were gently guided to the escape box and habituated there for 1 min. Mice were rotated in a trial for a total of 4 trials per day. Latency to enter the escape box was measured and analyzed to assess spatial memory learning ability.

On the day following the training session, the probe test with a closed target hole was performed for 3 min to assess memory retrieval based on (1) time spent in the target quadrant including the target hole, (2) latency to first approach to the target hole, and (3) primary errors (the number of error approaches before the first approach to the target hole) and total errors (the total number of error approaches during the probe test). The test was conducted only once per mouse. The detection zones of each hole were defined as the 7.5 cm in diameter circle including each hole.

The day after the probe test, a reversal test was conducted under the same conditions as the training session, except that the escape position was reversed 180 degrees. Mice were rotated in one trial for a total of 4 trials. Cognitive flexibility was assessed by the latency to enter the escape box.

To eliminate the influence of different activity levels on the performance, mice whose total active time in the probe test was within mean ± 2 standard deviations (SD) of that of Sham-WT mice were selected for analysis.

Statistical analysis

Statistical analysis was performed using Prism 10.4.1 (GraphPad). Student's *t*-test was used for statistical analysis between two groups (Control vs. mild AD, WT vs. App, and Sham-WT vs. Sham-App). One-way ANOVA

followed by Bonferroni's multiple comparison test was performed for three groups (Cortex vs. Microglia vs. Astrocytes). For four groups (Sham-WT vs. Cast-WT vs. Sham-App vs. Cast-App), two-way ANOVA with or without repeated measures was performed to evaluate the main effects of each factor and the interaction, followed by Bonferroni's multiple comparison test. Data are presented as means \pm SEMs. Statistical significance was defined as $p < 0.05$. Detailed results of the statistical analysis are summarized in **Supplementary Table 3**.

Results

Androgen receptor mRNA levels decreased in the precune of patients with early AD pathology and in isolated microglia of male *App*^{NL-G-F/NL-G-F} mice

Androgens exert their effects through androgen receptor (AR), which is widely expressed in the brains of humans^{40–42} and mice^{43,44}. To determine whether AR is associated with AD, we compared AR expression levels in the precune of patients with early AD pathology (mild AD) and non-ADs (controls) using quantitative PCR (qPCR). Postmortem human brains were selected based on Braak stage as determined by senile plaque (SP) and neurofibrillary tangle (NFT) levels as follows: 14 control brains defined by SP = 0–A, NFT = 0–II and 11 mild AD brains defined by SP = C, NFT = III–IV (Fig. 1a). Compare with controls, AR expression levels in mild AD brains were significantly lower in males (Fig. 1b) but not in females (Fig. 1c).

To verify whether AR expression levels are similarly decreased in the brain of male AD mouse model, we analyzed *App*^{NL-G-F/NL-G-F} (App) mice, which express humanized A β fragments with familial AD mutations at physiological levels. We performed qPCR on the cerebral cortices and isolated microglia from 8-month-old male wild-type (WT) and App mice (Fig. 1d). AR expression levels in the cerebral cortex did not differ between these mice (Fig. 1e); however, isolated microglia from App mice showed a significant decrease in AR expression levels compared with those from WT mice (Fig. 1f).

Collectively, these results suggest that AR/AR expression levels in the brains and microglia of males are altered by AD pathology.

Long-term castration downregulates neuroinflammation-related gene expression in glial cells of male *App*^{NL-G-F/NL-G-F} mice

To assess the effects of long-term systemic androgen deprivation on AD pathology, we performed sham operation or castration on 4-month-old male WT and App mice (Fig. 2a). App mice exhibit amyloid deposition at 2.5 months of age, gliosis at 3 months, and mild cognitive impairment at 6 months¹². We performed a behavioral test and tissue sampling at 18 months of age when these AD pathologies were well-advanced.

First, we examined the systemic effects of androgen deprivation, such as body, spleen, and testis weight changes. Body weight (BW) was similar across all groups at 18 months of age (Supplementary Fig. 1a). Spleen weight per BW showed no significant differences across all groups, although Sham-App mice tended to have lighter spleens compared with Sham-WT mice (FC = 0.54), which was slightly reversed by castration (Supplementary Fig. 1b). Testis weight per BW was significantly decreased (Supplementary Fig. 1c), whereas seminal vesicle (SV) weight per BW was significantly increased (Supplementary Fig. 1d) in Sham-App mice compared with Sham-WT mice. The castration group exhibited a significant decrease in SV size, reaching an invisible level. Given the sensitivity of SV weight to androgen levels⁴⁵, this reduction in SV size indicates effective androgen deprivation by castration.

To investigate whether long-term systemic androgen deprivation modulates neuroinflammation in male App mice, we analyzed cell type-specific gene expression in isolated microglia and astrocytes from male Sham- or Cast- WT and App mice at 18 months of age using qPCR (Fig. 2b). The high purity of MACS-isolated microglia and astrocytes was determined by measuring the expression levels of representative cell type-specific markers, such as the microglial marker *IBA1/Aif1*, glutamate/aspartate transporter 1 (GLAST)/*Slc1a3* as the astrocyte marker, the oligodendrocyte marker *Mbp*, and the neuronal marker *Tubb3* (Supplementary Fig. 2). In isolated microglia (Fig. 2c), AR expression levels were significantly downregulated in 18-month-old Sham-App mice compared with Sham-WT mice, similar to 8-month-old mice (Fig. 1f), whereas its levels were unaffected by castration. Upon measuring the expression levels of neuroinflammation-related genes, such as proinflammatory chemokines and cytokines (*Cxcl10*, *Ccl5*, and *Il6*), A1-astrocyte inducers (*Tnf*, *Il1a*, and *C1qa*), pan-activated microglial marker (*Cd68*), and a DAM marker (*Itgax*), all genes except *Il1a* showed significantly upregulated expression levels in Sham-App mice relative to Sham-WT mice (Fig. 2c and Supplementary Fig. 3a). Intriguingly, castration led to significantly reduced *Tnf* expression levels in App mice, although levels remained higher than those in Cast-WT mice. Similarly, *Il6* expression levels were significantly reduced by castration in App mice. However, the expression levels of homeostatic microglial marker (*Tmem119*) and anti-inflammatory microglial marker (CD206/*Mrc1*) were not altered by castration (Supplementary Fig. 3b, c). In isolated astrocytes (Fig. 2d), AR expression levels did not differ among groups. Upon measuring neuroinflammation-related gene expression levels in astrocytes, including a pan-astrocyte marker (*Gfap*), A1-astrocyte markers (*H2-D1* and *Psmb8*), and inflammatory regulators (*Stat3* and *Socs3*), we found that all gene expression levels were upregulated in Sham-App mice. Notably, *Socs3* expression levels were significantly decreased in Cast-App mice compared with Sham-App mice.

Taken together, these results indicate that long-term systemic androgen deprivation downregulates the expression levels of some neuroinflammation-related genes in isolated microglia and astrocytes of male App mice.

Long-term castration does not affect A β accumulation, gliosis, or dystrophic neurites in male *App*^{NL-G-F/NL-G-F} mice

To assess whether long-term systemic androgen deprivation exacerbates A β pathology and gliosis in App mice, we examined A β accumulation and a microglial marker IBA1 expression in the cerebral cortex, hippocampus,

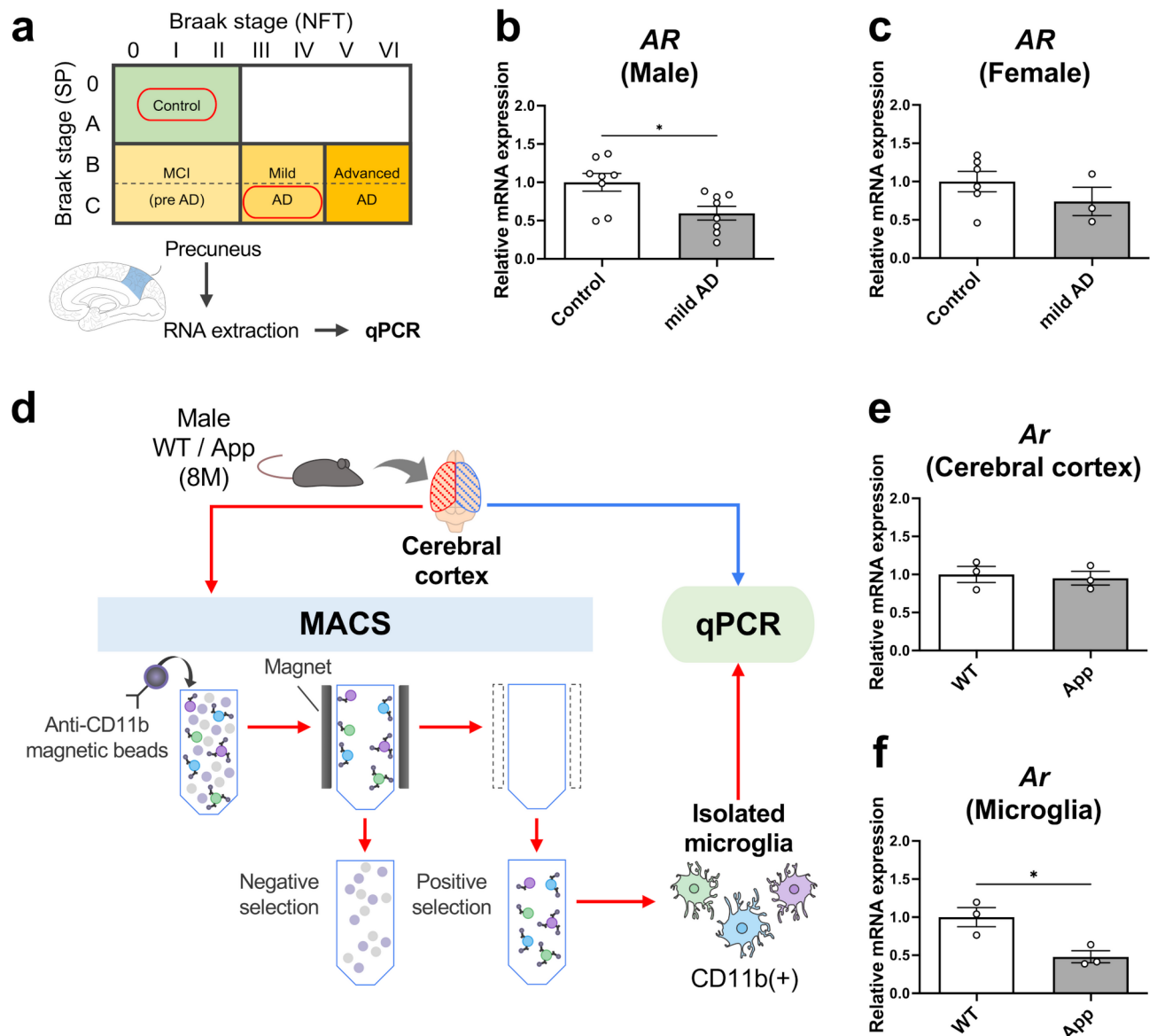


Fig. 1. *AR/Ar* mRNA levels are downregulated in the brains of male patients with early AD pathology and isolated microglia from male *App*^{NL-G-F/NL-G-F} mice. **(a)** Schematic of human brain sample selection based on Braak staging as determined according to senile plaque (SP) levels (0–C) and neurofibrillary tangle (NFT) levels (0–VI). non-AD (control): SP = 0–A, NFT = 0–II; the patients with early AD pathology (mild AD): SP = C, NFT = III–IV. Total RNA was extracted from the precuneus of control and mild AD samples for quantitative PCR (qPCR). **(b, c)** *AR* expression levels in the human precuneus determined via qPCR. Relative expression levels are plotted as means ± standard errors of means (SEMs). Data are shown for males **(b)** and females **(c)** [Control (*n* = 8) and mild AD (*n* = 8) in males; control (*n* = 6) and mild AD (*n* = 3) in females]. **(d)** Schematic of total RNA preparation from mouse cerebral cortices and microglia isolated via magnetic-activated cell sorting (MACS). Microglia were isolated from one-half of the cerebral cortices of 8-month-old male wild-type (WT) and *App*^{NL-G-F/NL-G-F} (*App*) mice via MACS. Total RNA was extracted from the remaining cerebral cortices and isolated microglia. **(e, f)** Relative *Ar* expression levels in mouse cerebral cortex **(e)** and isolated microglia **(f)** measured using qPCR. Data are presented as means ± SEMs [WT (*n* = 3) and *App* (*n* = 3)]. **p* < 0.05 and ***p* < 0.01 by Student's *t*-test **(b, c, e and f)**.

and amygdala using immunofluorescence in 18-month-old male Sham- or Cast- WT and *App* mice. In the cerebral cortex of Sham-WT mice, microglia with ramified morphology were observed and remained unchanged by castration. In the *App* group, Aβ accumulation significantly increased, accompanied by more IBA1-positive microglia with amoeboid morphology compared to the WT group (Fig. 3a). Quantitative analysis revealed that castration did not affect Aβ accumulation (Fig. 3d) or the expression of IBA1-positive microglia (Fig. 3e) in *App* mice. These results were consistent across other brain regions (Fig. 3b–e). We also analyzed the expression of microglial phagocytic marker CD68 in the cerebral cortex (Supplementary Fig. 4b). However, the

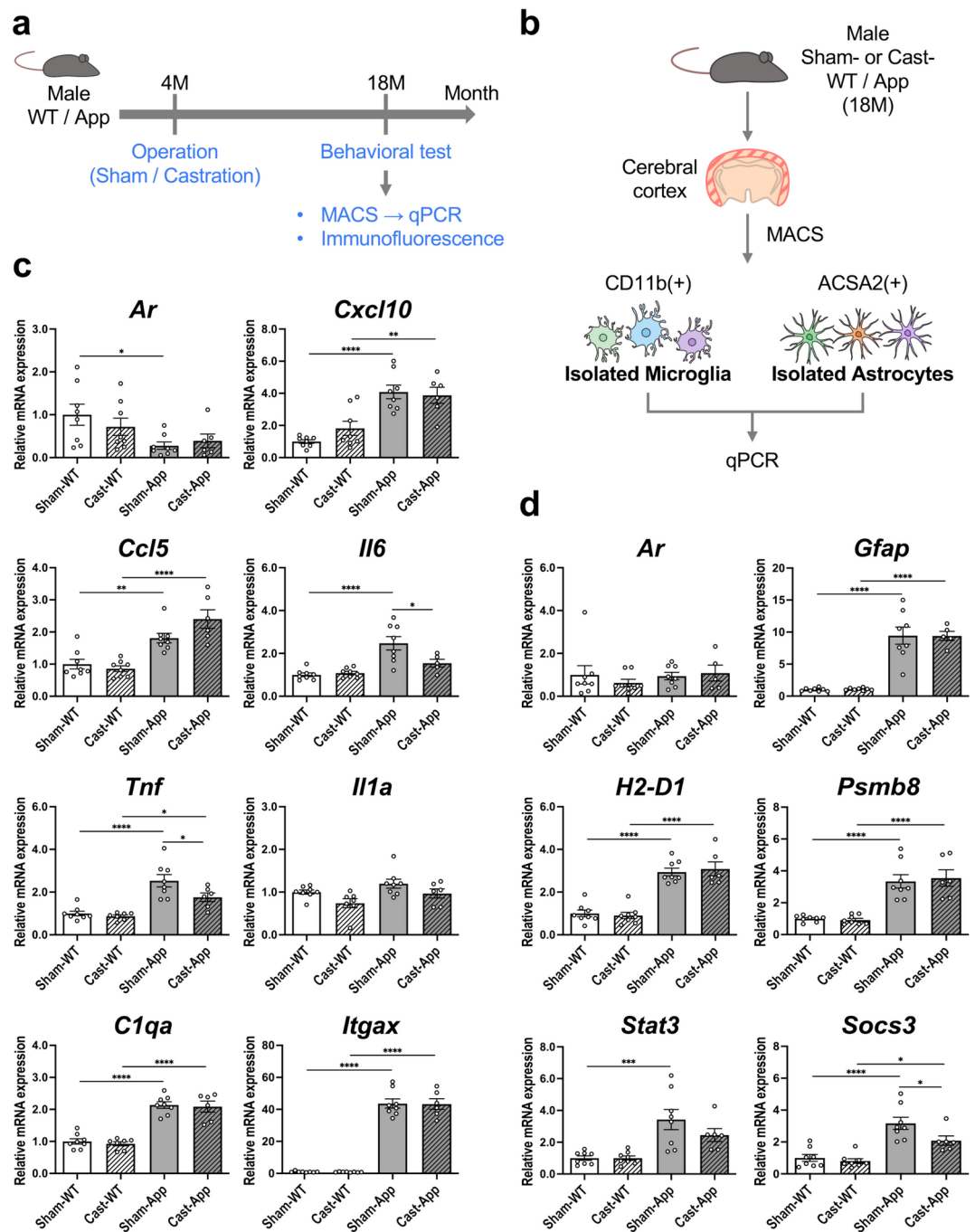


Fig. 2. Long-term castration alters neuroinflammatory-related gene expression in glial cells of *App^{NL-G-F/NL-G-F}* mice. **(a)** Schematic of long-term systemic androgen deprivation and subsequent behavioral, expression, and histological analyses in male WT and App mice. **(b)** Schematic protocol for microglia and astrocytes isolation from the cerebral cortices of 18-month-old male sham-operated (Sham-) or castrated (Cast-) WT and App mice via MACS, followed by gene expression analysis through qPCR [Sham-WT mice ($n=8$), Cast-WT mice ($n=7-8$), Sham-App mice ($n=8$), and Cast-App mice ($n=5-6$)]. **(c)** mRNA levels in isolated microglia from Sham- or Cast- WT and App mice measured using qPCR. Relative expression levels of *Ar*, proinflammatory chemokines/cytokines (*Cxcl10*, *Ccl5*, and *Il6*), A1-astrocyte inducers (*Tnf*, *Il1a*, and *C1qa*), and a DAM marker (*Itgax*) are presented as means \pm SEMs. **(d)** mRNA levels in astrocytes isolated from Sham- or Cast- WT and App mice determined via qPCR. Relative expression levels of *Ar*, a pan-astrocyte marker (*Gfap*), A1-astrocyte markers (*H2-D1* and *Psmb8*), and inflammatory regulators (*Stat3* and *Socs3*) are plotted as means \pm SEMs. * $p < 0.05$, ** $p < 0.01$, *** $p < 0.001$ and **** $p < 0.0001$ by two-way ANOVA with Bonferroni correction (c, d).

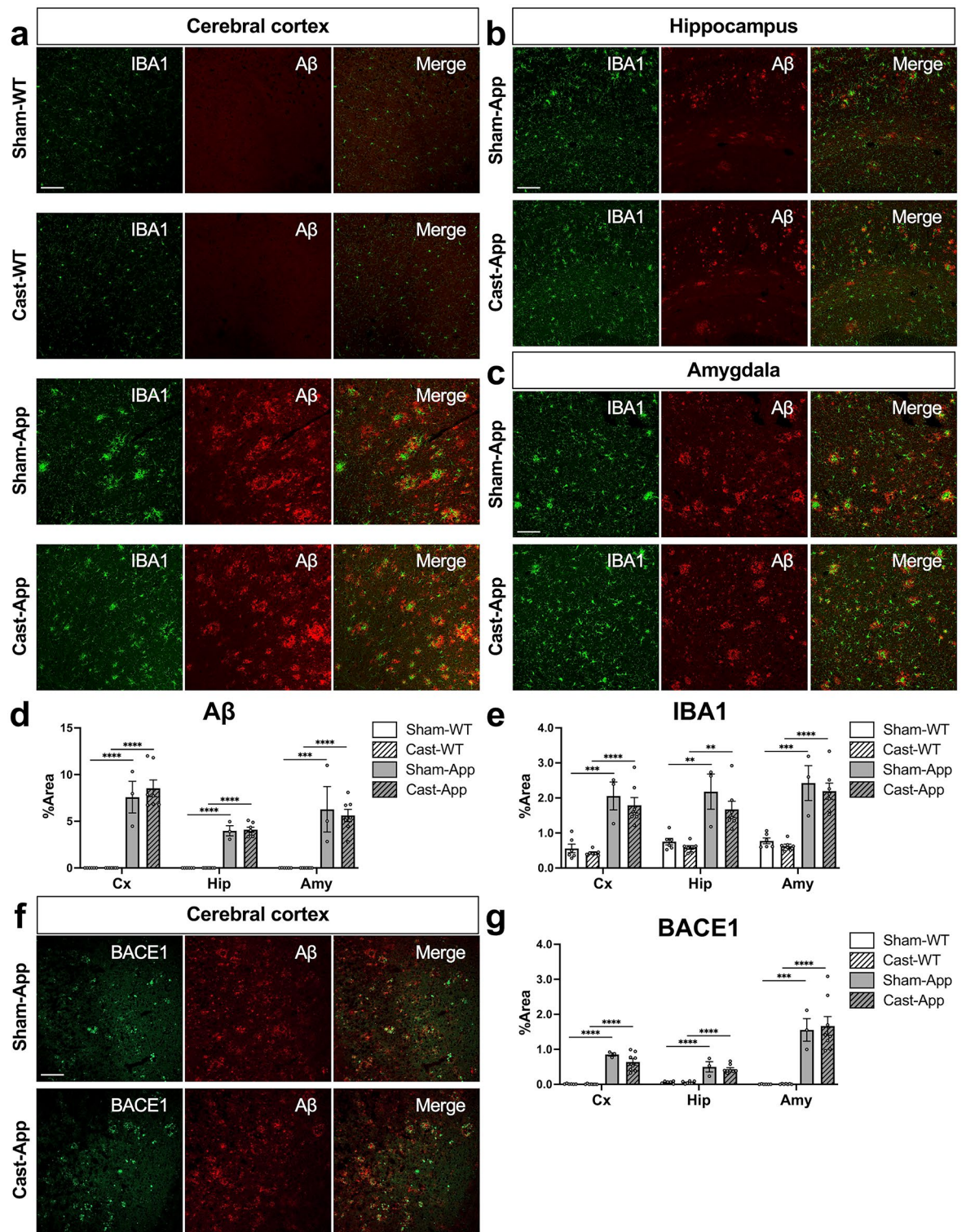


Fig. 3. Long-term castration does not affect A β pathology or dystrophic neurites in *App*^{NL-G-F/NL-G-F} mice. (a–c) Representative immunofluorescence images showing IBA1 (green) and A β (red) expression, along with merged images, in the cerebral cortex (a), hippocampus (b), and amygdala (c) of 18-month-old male Sham- or Cast- WT and App mice. Scale bars: 100 μ m. (d, e) Quantification of immunofluorescence images from (a–c). Percentage of immunopositive areas for A β (d) and IBA1 (e) in the cerebral cortex (Cx), hippocampus (Hip), and amygdala (Amy). f Representative immunofluorescence images showing BACE1 (green) and A β (red) expression, along with merged images, in the cerebral cortex of 18-month-old male Sham- or Cast- App mice. Scale bar: 100 μ m. (g) Quantification of immunofluorescence images from (f). Percentage of BACE1 immunopositive areas (f). Data are presented as means \pm SEMs (d, e and g) [Sham-WT mice ($n=6$), Cast-WT mice ($n=7$), Sham-App mice ($n=3$), and Cast-App mice ($n=7-8$); three sections quantified per mouse]. * $p < 0.05$, ** $p < 0.01$, *** $p < 0.001$ and **** $p < 0.0001$ by two-way ANOVA with Bonferroni correction.

number of CD68/IBA1 double-positive microglia surrounding A β plaques remained unchanged by castration (Supplementary Fig. 4c). This result is consistent with the qPCR result for *Cd68* mRNA expression levels (Supplementary Fig. 3a). These findings suggest that long-term systemic androgen deprivation does not impact A β accumulation or gliosis in male App mice.

Expression levels and activity of BACE1, involved in A β synthesis and synaptic function, are known to increase in the dystrophic presynaptic terminals of patients with AD and 5xFAD mice^{46–48}. Additionally, increasing testosterone levels have been shown to result in downregulated BACE1 expression and activity in male APP23 AD model mice⁴⁹. Therefore, to determine whether castration affects BACE1 levels, we costained for BACE1 and A β in App mice. Although BACE1 immunoreactivity was undetectable in WT mice, it was present around A β plaques in the cerebral cortex (Fig. 3f), hippocampus, and amygdala (Supplementary Fig. 4d) of App mice. However, castration did not alter the percentage of BACE1-positive staining (Fig. 3g). These results indicate that long-term systemic androgen deprivation does not affect BACE1 protein expression in male App mice.

Long-term castration does not affect cognitive function in male App^{NL-G-F/NL-G-F} mice

To determine whether long-term systemic androgen deprivation exacerbates cognitive dysfunction in male App mice, we assessed spatial learning and memory using the Barnes maze test, which evaluates hippocampal function, in 18-month-old WT and App mice with or without castration (Fig. 4a).

During the training session, a significant Day effect (Day1 vs. 2 vs. 3 vs. 4 vs. 5) was observed in the latency to reach the target hole (Fig. 4b). Although no Mouse effect (Sham-WT vs. Cast-WT vs. Sham-App vs. Cast-App) was observed, multiple comparison test showed significant differences between sham-operation and castration groups in both genotypes, respectively only on Day 1. These differences were not observed on subsequent days, suggesting that they may be attributed to the impact of castration on anxiety-related behaviors in the novel environment⁵⁰. This result indicates no difference in spatial learning across the four groups and that all groups completed learning by the last day of the training session.

In the probe test, all groups showed a preference for exploring the target quadrant over other quadrants. Sham-App mice spent significantly less time in the target quadrant compared with Sham-WT mice. Castration reversed this reduction in Sham-App mice, but the effect was not statistically significant (Fig. 4c). The latency for Sham-App mice to first approach to the target hole tended to be longer than that for Sham-WT mice (FC = 1.82), but all groups showed no significant differences (Fig. 4d). Primary errors (Fig. 4e) and total errors (Fig. 4f) were also measured, however, they did not differ between genotypes or between operations. These results suggest that male App mice exhibit cognitive impairment in spatial memory relative to male WT mice, but that this deficit is not significantly altered by castration. In the reversal test, no differences in latency were observed across all groups (Fig. 4g), indicating that male App mice retain cognitive flexibility, even after castration.

Discussion

In this study, we observed significantly lower *AR/Ar* expression levels in both male human mild AD precune and male App mouse brain microglia compared with their controls. Using castrated male App mice, we investigated the effects of long-term systemic androgen deprivation on AD phenotype and pathology, revealing that spatial memory impairment and A β accumulation remained unchanged in these mice, whereas several neuroinflammation-related genes were significantly downregulated in their isolated microglia and astrocytes.

We focused on the role of androgens in AD-related neuroinflammation. Although prior reports on microglial *AR/Ar* expression are inconsistent^{41,51–53}, we observed decreased *Ar* levels in microglia isolated from App mouse brains. *Ar* depletion was observed only in microglia, not in astrocytes or the cerebral cortex, and was unaffected by castration, suggesting that *Ar* expression in microglia may be regulated by a distinct mechanism from other cell types, independent of androgen levels. We interpret that reduced *Ar* expression in microglia of neurodegenerative disease models is linked to microglial activation. This is further supported by our previous RNA-seq data, which showed lower *Ar* levels in pathologically activated microglia isolated from SOD1^{G93A} ALS and rTg4510 tau model mice compared with their controls (Open RNA-seq data from Sobue et al.¹²). These findings suggest that *Ar* depletion in activated microglia may influence neuroinflammation in AD pathology.

The inflammatory role of androgens remains unclear, with both pro- and anti-inflammatory effects reported⁵⁴. For instance, Yang et al. described an anti-inflammatory role of androgens in the brains of lipopolysaccharide-treated male WT mice⁵⁵. Conversely, androgen blockade through castration⁵⁶ or myeloid-specific AR knockout in male mice⁵⁷ is known to reduce the expression of proinflammatory molecules, such as TNF- α and IL-6, in wound tissues and accelerate wound healing. These studies imply that the inflammatory role of androgens is likely to vary by tissue, cell type, and pathology. Few studies have investigated the inflammatory effects of androgens in AD model mice. In this study, we found that long-term castration reduced *Tnf* and *Il6* expression levels in microglia of male App mice, suggesting that androgens may promote inflammation in diseased microglia. However, the majority of microglial gene expression levels, including proinflammatory molecules, anti-inflammatory state markers, and microglial phagocytosis, remained unaltered in Cast-App mice. These findings suggest that the impact of androgen deprivation on microglial phenotypic changes is limited, and therefore, insufficient to alter the AD pathologies in male App mice. Furthermore, in isolated astrocytes, even though *Ar* expression levels did not differ across the test groups (Fig. 2d), *Socs3* expression levels were significantly decreased in Cast-App mice. As *Socs3* is upregulated by IL-6 via JAK/STAT signaling and inhibits IL-6 signaling through negative feedback⁵⁸, its downregulation in astrocytes may result from decreased *Il6* expression in microglia. This suggests that androgens may regulate microglia–astrocytes crosstalk, thereby modulating neuroinflammation.

Irrespective of neuroinflammatory changes, we initially expected that castration would affect cognitive dysfunction and A β aggregation in male App mice. However, no such changes were observed in the phenotype or pathology of Cast-App mice. In contrast, studies using 3xTg-AD mice⁵⁶ and APP/PS1 mice^{37,59} reported that castration exacerbated cognitive deficits and increased A β plaques. The discrepancy may be attributed

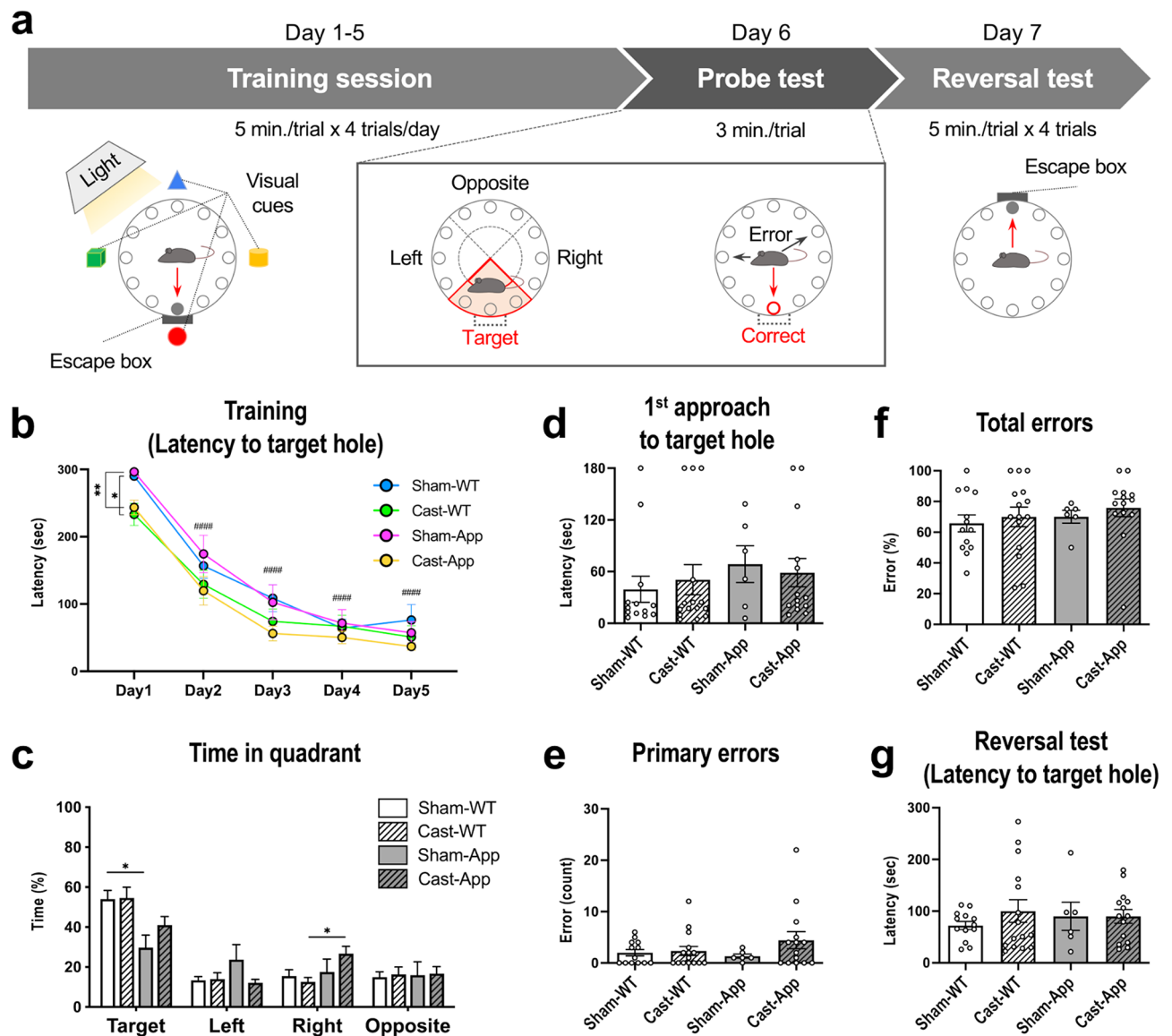


Fig. 4. Long-term systemic androgen deprivation does not affect cognitive function in *App^{NL-G-F/NL-G-F}* mice. **(a)** Experimental protocol for the Barnes maze test using 18-month-old male Sham- or Cast- WT and App mice [Sham-WT mice ($n = 13$), Cast-WT mice ($n = 15$), Sham-App mice ($n = 6$), and Cast-App mice ($n = 14$)]. **(b)** Latency to enter the target hole during the training session. Each plot represents the mean \pm SEM of four trials per group. Two-way repeated measures ANOVA with Bonferroni correction determined differences (* $p < 0.05$; between groups on each trial day, #### $p < 0.0001$: vs. Day1 in all groups). **(c–f)** Spatial memory was assessed during the probe test period based on the percentage of time spent in quadrant area **(c)**, latency to first approach to the target hole **(d)**, the number of primary errors **(e)**, and the percentage of total errors **(f)**. Data are presented as means \pm SEMs. * $p < 0.05$ by two-way ANOVA with Bonferroni correction. **(g)** Latency to enter the target hole during the reversal test period. Each graph shows the means \pm SEMs of the latency over four trials per group. Two-way ANOVA with Bonferroni correction determined differences.

to different AD mouse models used in each study. In fact, Zhang et al. reported that ADT, a combination of castration and ADT drugs, did not affect A β burden in male App mice with prostate tumors⁶⁰, aligning with our results. Additionally, although ovariectomy is known to markedly alter A β pathology in other AD mouse models^{19–21}, its impact on female App mice was limited⁶¹. These findings suggest that gonadectomy has minimal influence on A β accumulation in App mice and that the response of brain A β pathology to peripheral sex steroid changes may depend on the type of mouse model used.

Although the previous study reported that App mice showed a modest cognitive decline at 6 months of age^{39,62}, we confirmed that App mice showed a decline in cognitive function as measured by the Barnes maze test at 11 months of age⁶³. Based on these findings, we decided to analyze the impact of castration on male App mice at 18 months of age, when they should have advanced phenotype and pathology. It should be noted that our results in castrated 18-month-old App mice were possibly influenced by the combination of castration and

aging, as the systemic testosterone levels are presumably reduced in aged rodents. Although we did not directly confirm whether testosterone levels were altered by aging, we observed that the seminal vesicle weight, which is known to respond to testosterone levels⁴⁵, was preserved in 18-month-old sham-operated mice but not in castrated mice. This result suggests that testosterone levels are likely to be maintained at sufficient levels in sham-operated mice compared with castrated mice even at 18 months of age. Therefore, although it cannot be completely excluded, the effect of aging on our experimental results seems to be limited. Additionally, the possibility that AD pathologies might reach a plateau at 18 months of age, making the effects of castration difficult to detect, should also be considered as a limitation. In order to obtain clearer results of castration or to compare with early AD pathology in humans, a time course analysis of androgen deprivation in AD mice, including earlier time points, is a future challenge for this study.

Our analysis revealed significantly lower AR expression levels in male human mild AD precuneus compared with controls, which supports previous studies reporting that brain and serum testosterone levels are decreased in male patients with AD relative to noncognitively impaired individuals^{22,23}. However, a study by Ishunina et al. reported lower AR expression in the basal forebrain of female AD cases⁶⁴. The difference between our findings and those of Ishunina et al. may be due to variations in analysis (mRNA levels vs. immunohistochemistry), brain regions, or pathological stages. As only a few studies have focused on AR expression in AD brains, further research with a large number of AD cases is required to clarify the relationships between AR expression and disease stage, sex differences, and distribution in the brain.

Our study has several limitations. First, since we focused on neuroinflammation in App mice, we did not examine the neuronal contributions of AR signaling. Androgens modulate spine density⁶⁵, synaptic plasticity⁶⁶, and neurogenesis⁶⁷ in the hippocampus through neuronal AR. These neuroprotective effects of androgens have also been observed in APP/PS1 mice³⁷ and APP23 mice⁴⁹, but owing to differences in AD mouse models, further research is needed to verify these effects in App mice. Second, a limited number of candidate glia-related genes were analyzed in App mice with castration. The use of comprehensive gene and cytokine expression analysis will provide a complete picture of neuroinflammation modulation by androgen deprivation in AD mouse model. Third, the number of mice for immunofluorescence was not sufficient, which may have an impact on our conclusion of insufficient effects of castration. Finally, castration also affects other hormone levels, follicle stimulating hormone and luteinizing hormone. The potential influence of these hormones, which have been associated with AD pathologies^{68–70}, should be considered when interpreting our findings. We also raise the further issue to be addressed. While we have focused on the effect of androgen on neuroinflammation under A β pathology, whether androgens influence tau pathology remains an open question. Activated glial cells and released proinflammatory molecules also exacerbate tau hyperphosphorylation, aggregation, and propagation⁷¹. The impact of long-term castration on neuroinflammation in tau pathology needs to be investigated.

In conclusion, our study demonstrates that androgen deprivation affects neuroinflammation in AD pathology. Additionally, we provide new evidence that androgens exert proinflammatory action on microglia, alongside the previously reported anti-inflammatory effects. However, the changes in neuroinflammation induced by long-term systemic androgen deprivation are insufficient to alter A β accumulation or cognitive dysfunction in male App mice, a genetic model of AD.

Data availability

All data generated or analyzed during this study are included in this published article and/or the Supplementary Materials.

Received: 5 October 2024; Accepted: 15 April 2025

Published online: 27 April 2025

References

1. Bellenguez, C. et al. New insights into the genetic etiology of Alzheimer's disease and related dementias. *Nat. Genet.* **54**, 412–436. <https://doi.org/10.1038/s41588-022-01024-z> (2022).
2. Kunkle, B. W. et al. Genetic meta-analysis of diagnosed Alzheimer's disease identifies new risk loci and implicates A β , Tau, immunity and lipid processing. *Nat. Genet.* **51**, 414–430. <https://doi.org/10.1038/s41588-019-0358-2> (2019).
3. Jansen, I. E. et al. Genome-wide meta-analysis identifies new loci and functional pathways influencing Alzheimer's disease risk. *Nat. Genet.* **51**, 404–413. <https://doi.org/10.1038/s41588-018-0311-9> (2019).
4. Heneka, M. T. et al. Neuroinflammation in Alzheimer's disease. *Lancet Neurol.* **14**, 388–405. [https://doi.org/10.1016/S1474-4422\(15\)70016-5](https://doi.org/10.1016/S1474-4422(15)70016-5) (2015).
5. De Strooper, B. & Karran, E. The cellular phase of Alzheimer's disease. *Cell* **164**, 603–615. <https://doi.org/10.1016/j.cell.2015.12.056> (2016).
6. Davalos, D. et al. ATP mediates rapid microglial response to local brain injury in vivo. *Nat. Neurosci.* **8**, 752–758. <https://doi.org/10.1038/nn1472> (2005).
7. Nimmerjahn, A., Kirchhoff, F. & Helmchen, F. Resting microglial cells are highly dynamic surveillants of brain parenchyma in vivo. *Science* **308**, 1314–1318. <https://doi.org/10.1126/science.1110647> (2005).
8. Wang, W. Y., Tan, M. S., Yu, J. T. & Tan, L. Role of pro-inflammatory cytokines released from microglia in Alzheimer's disease. *Ann. Transl. Med.* **3**, 136. <https://doi.org/10.3978/j.issn.2305-5839.2015.03.49> (2015).
9. Leng, F. & Edison, P. Neuroinflammation and microglial activation in Alzheimer disease: where do we go from here? *Nat. Rev. Neurol.* **17**, 157–172. <https://doi.org/10.1038/s41582-020-00435-y> (2021).
10. Sierra, A., Abiega, O., Shahraz, A. & Neumann, H. Janus-faced microglia: beneficial and detrimental consequences of microglial phagocytosis. *Front. Cell. Neurosci.* **7**, 6. <https://doi.org/10.3389/fncel.2013.00006> (2013).
11. Keren-Shaul, H. et al. A Unique Microglia Type Associated with Restricting Development of Alzheimer's Disease. *Cell* **169**, 1276–1290.e1217. <https://doi.org/10.1016/j.cell.2017.05.018> (2017).
12. Sobue, A. et al. Microglial gene signature reveals loss of homeostatic microglia associated with neurodegeneration of Alzheimer's disease. *Acta Neuropathol. Commun.* **9**, 1. <https://doi.org/10.1186/s40478-020-01099-x> (2021).

13. Liddel, S. A. et al. Neurotoxic reactive astrocytes are induced by activated microglia. *Nature* **541**, 481–487. <https://doi.org/10.1038/nature21029> (2017).
14. Matias, I., Morgado, J. & Gomes, F. C. A. Astrocyte Heterogeneity: Impact to Brain Aging and Disease. *Front. Aging Neurosci.* **11**, 59. <https://doi.org/10.3389/fnagi.2019.00059> (2019).
15. Seshadri, S. et al. Lifetime risk of dementia and Alzheimer's disease. The impact of mortality on risk estimates in the Framingham study. *Neurology* **49**, 1498–1504. <https://doi.org/10.1212/wnl.49.6.1498> (1997).
16. Niu, H., Álvarez-Alvarez, I., Guillén-Grima, F. & Aguinaga-Ontoso, I. Prevalence and incidence of Alzheimer's disease in Europe: A meta-analysis. *Neurologia* **32**, 523–532. <https://doi.org/10.1016/j.nrl.2016.02.016> (2017).
17. Beam, C. R. et al. Differences Between Women and Men in Incidence Rates of Dementia and Alzheimer's Disease. *J. Alzheimers Dis.* **64**, 1077–1083. <https://doi.org/10.3233/JAD-180141> (2018).
18. Tang, M. X. et al. Effect of oestrogen during menopause on risk and age at onset of Alzheimer's disease. *Lancet* **348**, 429–432. [https://doi.org/10.1016/S0140-6736\(96\)03356-9](https://doi.org/10.1016/S0140-6736(96)03356-9) (1996).
19. Luo, M. et al. Estrogen deficiency exacerbates learning and memory deficits associated with glucose metabolism disorder in APP/PS1 double transgenic female mice. *Genes Dis.* **9**, 1315–1331. <https://doi.org/10.1016/j.gendis.2021.01.007> (2022).
20. Hou, Y. et al. Biochanin A alleviates cognitive impairment and hippocampal mitochondrial damage in ovariectomized APP/PS1 mice. *Phytomedicine* **100**, 154056. <https://doi.org/10.1016/j.phymed.2022.154056> (2022).
21. Carroll, J. C. et al. Progesterone and Estrogen Regulate Alzheimer-Like Neuropathology in Female 3xTg-AD Mice. *J. Neurosci.* **27**, 13357–13365. <https://doi.org/10.1523/JNEUROSCI.2718-07.2007> (2007).
22. Hogervorst, E. et al. Serum total testosterone is lower in men with Alzheimer's disease. *Neuro Endocrinol. Lett.* **22**, 163–168 (2001).
23. Rosario, E. R., Chang, L., Head, E. H., Stanczyk, F. Z. & Pike, C. J. Brain levels of sex steroid hormones in men and women during normal aging and in Alzheimer's disease. *Neurobiol. Aging*. **32**, 604–613. <https://doi.org/10.1016/j.neurobiolaging.2009.04.008> (2011).
24. Jhan, J. H., Yang, Y. H., Chang, Y. H., Guu, S. J. & Tsai, C. C. Hormone therapy for prostate cancer increases the risk of Alzheimer's disease: a nationwide 4-year longitudinal cohort study. *Aging Male*. **20**, 33–38. <https://doi.org/10.1080/13685538.2016.1271782> (2017).
25. Jayadevappa, R. et al. Association Between Androgen Deprivation Therapy Use and Diagnosis of Dementia in Men With Prostate Cancer. *JAMA Netw. Open*. **2**, e196562. <https://doi.org/10.1001/jamanetworkopen.2019.6562> (2019).
26. Kim, J. W. et al. Androgen Deprivation Therapy in Patients with Prostate Cancer is Associated with the Risk of Subsequent Alzheimer's Disease but Not with Vascular Dementia. *World J. Mens Health*. **40**, 481–489. <https://doi.org/10.5534/wjmh.210019> (2022).
27. Loneragan, P. E. et al. Androgen Deprivation Therapy and the Risk of Dementia after Treatment for Prostate Cancer. *J. Urol.* **207**, 832–840. <https://doi.org/10.1097/JU.0000000000002335> (2022).
28. Hinojosa-Gonzalez, D. E. et al. Androgen deprivation therapy for prostate cancer and neurocognitive disorders: a systematic review and meta-analysis. *Prostate Cancer Prostatic Dis.* **27**, 507–519. <https://doi.org/10.1038/s41391-023-00785-w> (2024).
29. Nead, K. T., Sinha, S. & Nguyen, P. L. Androgen deprivation therapy for prostate cancer and dementia risk: a systematic review and meta-analysis. *Prostate Cancer Prostatic Dis.* **20**, 259–264. <https://doi.org/10.1038/pcan.2017.10> (2017).
30. Sari Motlagh, R. et al. The Risk of New Onset Dementia and/or Alzheimer Disease among Patients with Prostate Cancer Treated with Androgen Deprivation Therapy: A Systematic Review and Meta-Analysis. *J. Urol.* **205**, 60–67. <https://doi.org/10.1097/JU.0000000000001341> (2021).
31. Khosrow-Khavar, F., Rej, S., Yin, H., Aprikian, A. & Azoulay, L. Androgen Deprivation Therapy and the Risk of Dementia in Patients With Prostate Cancer. *J. Clin. Oncol.* **35**, 201–207. <https://doi.org/10.1200/JCO.2016.69.6203> (2017).
32. Baik, S. H., Kury, F. S. P. & McDonald, C. J. Risk of Alzheimer's Disease Among Senior Medicare Beneficiaries Treated With Androgen Deprivation Therapy for Prostate Cancer. *J. Clin. Oncol.* **35**, 3401–3409. <https://doi.org/10.1200/JCO.2017.72.6109> (2017).
33. Kim, Y. A., Kim, S. H., Joung, J. Y., Yang, M. S. & Back, J. H. The Insignificant Correlation between Androgen Deprivation Therapy and Incidence of Dementia Using an Extension Survival Cox Hazard Model and Propensity-Score Matching Analysis in a Retrospective, Population-Based Prostate Cancer Registry. *Cancers (Basel)*. **14** <https://doi.org/10.3390/cancers14112705> (2022).
34. Sun, M. et al. Cognitive Impairment in Men with Prostate Cancer Treated with Androgen Deprivation Therapy: A Systematic Review and Meta-Analysis. *J. Urol.* **199**, 1417–1425. <https://doi.org/10.1016/j.juro.2017.11.136> (2018).
35. Liu, J. M. et al. Association between Androgen Deprivation Therapy and Risk of Dementia in Men with Prostate Cancer. *Cancers*. **13**. <https://doi.org/10.3390/cancers13153861> (2021).
36. Rosario, E. R., Carroll, J. C., Oddo, S., LaFerla, F. M. & Pike, C. J. Androgens regulate the development of neuropathology in a triple transgenic mouse model of Alzheimer's disease. *J. Neurosci.* **26**, 13384–13389. <https://doi.org/10.1523/JNEUROSCI.2514-06.2006> (2006).
37. Song, L. et al. ZIP9 mediates the effects of DHT on learning, memory and hippocampal synaptic plasticity of male Tfm and APP/PS1 mice. *Front. Endocrinol. (Lausanne)*. **14**, 1139874. <https://doi.org/10.3389/fendo.2023.1139874> (2023).
38. Braak, H. & Braak, E. Neuropathological staging of Alzheimer-related changes. *Acta Neuropathol.* **82**, 239–259. <https://doi.org/10.1007/BF00308809> (1991).
39. Saito, T. et al. Single App knock-in mouse models of Alzheimer's disease. *Nat. Neurosci.* **17**, 661–663. <https://doi.org/10.1038/nn.3697> (2014).
40. Sarrieau, A. et al. Androgen binding sites in human temporal cortex. *Neuroendocrinology* **51**, 713–716. <https://doi.org/10.1159/000125415> (1990).
41. Puy, L. et al. Immunocytochemical detection of androgen receptor in human temporal cortex characterization and application of polyclonal androgen receptor antibodies in frozen and paraffin-embedded tissues. *J. Steroid Biochem. Mol. Biol.* **55**, 197–209. [https://doi.org/10.1016/0960-0760\(95\)00165-v](https://doi.org/10.1016/0960-0760(95)00165-v) (1995).
42. Fernández-Guasti, A., Kruijver, F. P., Fodor, M. & Swaab, D. F. Sex differences in the distribution of androgen receptors in the human hypothalamus. *J. Comp. Neurol.* **425**, 422–435. [https://doi.org/10.1002/1096-9861\(20000925\)425:3%3C422::AID-CNE7%3E3.0.CO;2-H](https://doi.org/10.1002/1096-9861(20000925)425:3%3C422::AID-CNE7%3E3.0.CO;2-H) (2000).
43. Cara, A. L., Henson, E. L., Beekly, B. G. & Elias, C. F. Distribution of androgen receptor mRNA in the prepubertal male and female mouse brain. *J. Neuroendocrinol.* **33**, e13063. <https://doi.org/10.1111/jne.13063> (2021).
44. Juntti, S. A. et al. The androgen receptor governs the execution, but not programming, of male sexual and territorial behaviors. *Neuron* **66**, 260–272. <https://doi.org/10.1016/j.neuron.2010.03.024> (2010).
45. Yoo, Y. E. & Ko, C. P. Dihydrotestosterone ameliorates degeneration in muscle, axons and motoneurons and improves motor function in amyotrophic lateral sclerosis model mice. *PLoS One*. **7**, e37258. <https://doi.org/10.1371/journal.pone.0037258> (2012).
46. Kandalepas, P. C. et al. The Alzheimer's β -secretase BACE1 localizes to normal presynaptic terminals and to dystrophic presynaptic terminals surrounding amyloid plaques. *Acta Neuropathol.* **126**, 329–352. <https://doi.org/10.1007/s00401-013-1152-3> (2013).
47. Zhang, X. M. et al. Beta-secretase-1 elevation in transgenic mouse models of Alzheimer's disease is associated with synaptic/axonal pathology and amyloidogenesis: implications for neuritic plaque development. *Eur. J. Neurosci.* **30**, 2271–2283. <https://doi.org/10.1111/j.1460-9568.2009.07017.x> (2009).
48. Sadleir, K. R. et al. Presynaptic dystrophic neurites surrounding amyloid plaques are sites of microtubule disruption, BACE1 elevation, and increased A β generation in Alzheimer's disease. *Acta Neuropathol.* **132**, 235–256. <https://doi.org/10.1007/s00401-016-1558-9> (2016).

49. McAllister, C. et al. Genetic targeting aromatase in male amyloid precursor protein transgenic mice down-regulates beta-secretase (BACE1) and prevents Alzheimer-like pathology and cognitive impairment. *J. Neurosci.* **30**, 7326–7334. <https://doi.org/10.1523/JNEUROSCI.1180-10.2010> (2010).
50. Boivin, J. R., Piekarski, D. J., Wahlberg, J. K. & Wilbrecht, L. Age, sex, and gonadal hormones differently influence anxiety- and depression-related behavior during puberty in mice. *Psychoneuroendocrinology* **85**, 78–87. <https://doi.org/10.1016/j.psychneuen.2017.08.009> (2017).
51. García-Ovejero, D., Veiga, S., García-Segura, L. M. & DonCarlos, L. L. Glial expression of estrogen and androgen receptors after rat brain injury. *J. Comp. Neurol.* **450**, 256–271. <https://doi.org/10.1002/cne.10325> (2002).
52. Finley, S. K. & Kritzer, M. F. Immunoreactivity for intracellular androgen receptors in identified subpopulations of neurons, astrocytes and oligodendrocytes in primate prefrontal cortex. *J. Neurobiol.* **40**, 446–457 (1999).
53. Sierra, A., Gottfried-Blackmore, A., Milner, T. A., McEwen, B. S. & Bulloch, K. Steroid hormone receptor expression and function in microglia. *Glia* **56**, 659–674. <https://doi.org/10.1002/glia.20644> (2008).
54. Vancolen, S., Sébire, G. & Robaire, B. Influence of androgens on the innate immune system. *Andrology* **11**, 1237–1244. <https://doi.org/10.1111/andr.13416> (2023).
55. Yang, L. et al. Neuroprotection by dihydrotestosterone in LPS-induced neuroinflammation. *Neurobiol. Dis.* **140**, 104814. <https://doi.org/10.1016/j.nbd.2020.104814> (2020).
56. Ashcroft, G. S. & Mills, S. J. Androgen receptor-mediated inhibition of cutaneous wound healing. *J. Clin. Invest.* **110**, 615–624. <https://doi.org/10.1172/JCI15704> (2002).
57. Lai, J. J. et al. Monocyte/macrophage androgen receptor suppresses cutaneous wound healing in mice by enhancing local TNF- α expression. *J. Clin. Invest.* **119**, 3739–3751. <https://doi.org/10.1172/JCI39335> (2009).
58. Babon, J. J., Varghese, L. N. & Nicola, N. A. Inhibition of IL-6 family cytokines by SOCS3. *Semin Immunol.* **26**, 13–19. <https://doi.org/10.1016/j.smim.2013.12.004> (2014).
59. Cao, J. et al. Androgen deprivation exacerbates AD pathology by promoting the loss of microglia in an age-dependent manner. *Life Sci.* **355**, 122973. <https://doi.org/10.1016/j.lfs.2024.122973> (2024).
60. Zhang, C. et al. Androgen deprivation therapy exacerbates Alzheimer's-associated cognitive decline via increased brain immune cell infiltration. *Sci. Adv.* **10**, eadn8709. <https://doi.org/10.1126/sciadv.adn8709> (2024).
61. Demetriou, A. et al. ER β mediates sex-specific protection in the *App^{NL-G-F}* mouse model of Alzheimer's disease. *BioRxiv* <https://doi.org/10.1101/2024.07.22.604543> (2024).
62. Wang, S. et al. Age-dependent behavioral and metabolic assessment of *App^{NL-G-F/NL-G-F}* Knock-in (KI) Mice. *Front. Mol. Neurosci.* **15**, 909989. <https://doi.org/10.3389/fnmol.2022.909989> (2022).
63. Sobue, A. et al. Microglial cannabinoid receptor type II stimulation improves cognitive impairment and neuroinflammation in Alzheimer's disease mice by controlling astrocyte activation. *Cell. Death Dis.* **15**, 858. <https://doi.org/10.1038/s41419-024-07249-6> (2024).
64. Ishunina, T. A., Fisser, B. & Swaab, D. F. Sex differences in androgen receptor immunoreactivity in basal forebrain nuclei of elderly and Alzheimer patients. *Exp. Neurol.* **176**, 122–132. <https://doi.org/10.1006/exnr.2002.7907> (2002).
65. Leranthy, C., Petnehazy, O. & MacLusky, N. J. Gonadal hormones affect spine synaptic density in the CA1 hippocampal subfield of male rats. *J. Neurosci.* **23**, 1588–1592. <https://doi.org/10.1523/JNEUROSCI.23-05-01588.2003> (2003).
66. Pan, W. et al. Effects of dihydrotestosterone on synaptic plasticity of the hippocampus in mild cognitive impairment male SAMP8 mice. *Exp. Ther. Med.* **12**, 1455–1463. <https://doi.org/10.3892/etm.2016.3470> (2016).
67. Hamson, D. K. et al. Androgens increase survival of adult-born neurons in the dentate gyrus by an androgen receptor-dependent mechanism in male rats. *Endocrinology* **154**, 3294–3304. <https://doi.org/10.1210/en.2013-1129> (2013).
68. Xiong, J. et al. FSH Blockade improves cognition in mice with Alzheimer's disease. *Nature* **603**, 470–476. <https://doi.org/10.1038/s41586-022-04463-0> (2022).
69. Lin, J. et al. Genetic ablation of luteinizing hormone receptor improves the amyloid pathology in a mouse model of Alzheimer disease. *J. Neuropathol. Exp. Neurol.* **69**, 253–261. <https://doi.org/10.1097/NEN.0b013e3181d072cf> (2010).
70. Verdile, G. et al. Associations between gonadotropins, testosterone and β amyloid in men at risk of Alzheimer's disease. *Mol. Psychiatry* **19**, 69–75. <https://doi.org/10.1038/mp.2012.147> (2014).
71. Chen, Y. & Yu, Y. Tau and neuroinflammation in Alzheimer's disease: interplay mechanisms and clinical translation. *J. Neuroinflammation* **20**, 165. <https://doi.org/10.1186/s12974-023-02853-3> (2023).

Acknowledgements

KM is supported by the “Nagoya University Interdisciplinary Frontier Fellowship” supported by Nagoya University and JST, the establishment of university fellowships towards the creation of science technology innovation, Grant Number JPMJFS2120. The authors thank the Center for Animal Research and Education (CARE) at Nagoya University for technical support for animal experiments.

Author contributions

KM, AS, and KY designed the study. KM and AS performed the experiments with support from OK. SM and YS selected and provided the post-mortem brain tissues. TS and TCS provided the *App^{+/NL-G-F}* mice and critical inputs. KM, AS, and KY interpreted the data. KM and KY wrote the manuscript with approval from all authors.

Funding

This work was supported by Grant-in-Aid for Scientific Research JP22H04923 (CoBiA) (Y.S., S.M.) from the Japan Society for the Promotion of Science (JSPS), AMED under Grant Numbers JP24wm0425014 (K.Y.) and JP21wm0425019 (Y.S., S.M.), Moonshot R&D from Japan Science and Technology Agency (JPMJMS2024 to K.Y.), MHLW Research on rare and intractable diseases Program Grant Number, JPMH23FC1008 (Y.S.), and Integrated Research Initiative for Living Well with Dementia (IRIDE) of the Tokyo Metropolitan Institute for Geriatrics and Gerontology IRIDE (Y.S.).

Declarations

Competing interests

The authors declare no competing interests.

Additional information

Supplementary Information The online version contains supplementary material available at <https://doi.org/10.1038/s41598-025-98825-z>.

Correspondence and requests for materials should be addressed to K.Y.

Reprints and permissions information is available at www.nature.com/reprints.

Publisher's note Springer Nature remains neutral with regard to jurisdictional claims in published maps and institutional affiliations.

Open Access This article is licensed under a Creative Commons Attribution-NonCommercial-NoDerivatives 4.0 International License, which permits any non-commercial use, sharing, distribution and reproduction in any medium or format, as long as you give appropriate credit to the original author(s) and the source, provide a link to the Creative Commons licence, and indicate if you modified the licensed material. You do not have permission under this licence to share adapted material derived from this article or parts of it. The images or other third party material in this article are included in the article's Creative Commons licence, unless indicated otherwise in a credit line to the material. If material is not included in the article's Creative Commons licence and your intended use is not permitted by statutory regulation or exceeds the permitted use, you will need to obtain permission directly from the copyright holder. To view a copy of this licence, visit <http://creativecommons.org/licenses/by-nc-nd/4.0/>.

© The Author(s) 2025, corrected publication 2025